

---

01 Jan 1985

## Raman Studies Of Heavily Implanted, Dye-laser-annealed GaAs

H. D. Yao

A. Compaan

Edward Boyd Hale

Missouri University of Science and Technology, ehale@mst.edu

Follow this and additional works at: [https://scholarsmine.mst.edu/phys\\_facwork](https://scholarsmine.mst.edu/phys_facwork)

 Part of the [Physics Commons](#)

---

### Recommended Citation

H. D. Yao et al., "Raman Studies Of Heavily Implanted, Dye-laser-annealed GaAs," *Solid State Communications*, vol. 56, no. 8, pp. 677 - 680, Elsevier, Jan 1985.

The definitive version is available at [https://doi.org/10.1016/0038-1098\(85\)90777-X](https://doi.org/10.1016/0038-1098(85)90777-X)

This Article - Journal is brought to you for free and open access by Scholars' Mine. It has been accepted for inclusion in Physics Faculty Research & Creative Works by an authorized administrator of Scholars' Mine. This work is protected by U. S. Copyright Law. Unauthorized use including reproduction for redistribution requires the permission of the copyright holder. For more information, please contact [scholarsmine@mst.edu](mailto:scholarsmine@mst.edu).



### RAMAN STUDIES OF HEAVILY IMPLANTED, DYE-LASER-ANNEALED GaAs

H.D. Yao & A. Compaan  
Department of Physics, Kansas State University, Manhattan, KS 66506  
U.S.A.

E.B. Hale  
Department of Physics and Materials Research Institute,  
University of Missouri-Rolla, Rolla, MO 65401 U.S.A.

Received September 2, 1985, by M. Cardona

Raman scattering is used to study the annealing behavior produced by 10 nsec, 565 nm dye laser pulses in high dose ion-implanted GaAs. Samples were prepared with Sn and Cd implantations of 2, 5, and  $10 \times 10^{15}/\text{cm}^2$ . The Raman spectra indicate that the threshold for epitaxial growth lies between 0.2 - 0.3 J/cm<sup>2</sup>. Best carrier activation (~2%), however, is achieved at ~1.6 J/cm<sup>2</sup> for the Sn-implanted sample (n-type). For Cd implantation the electrical activation appears to be very high (> 50%) for low pulse energies ( $\leq 0.3 \text{ J/cm}^2$ ) but decreases for higher pulse energies.

Raman scattering has proved to be a very useful nondestructive technique for studying doped GaAs over a broad range of carrier concentrations. At moderate dopant densities coupled phonon-plasmon modes have been used to obtain carrier concentrations and carrier mobilities and to study surface depletion layers. Ion-implantation-induced or laser-induced damage and polycrystalline grain size also influence the Raman spectrum. Recently it has been found that at the very high dopant densities ( $1 - 9 \times 10^{19}/\text{cm}^3$ ) achievable in Zn-doped GaAs, ionized acceptor scattering also induces large effects on the phonon-Raman spectrum. By suitably choosing laser wavelength, the Raman probe depth can be adjusted from ~1  $\mu\text{m}$  to as little as 0.01  $\mu\text{m}$  in GaAs. Raman scattering also can provide high transverse spatial resolution (~1-100  $\mu\text{m}$ ). Partly for these reasons Raman scattering has been used by several groups to study laser-annealed semiconductors, especially GaAs.

In this paper we report on the use of Raman scattering to monitor the progress of pulsed dye laser annealing of high dose ion-implanted GaAs. The Raman spectra provide estimates of epitaxial growth threshold (~0.3 J/cm<sup>2</sup>), carrier activation and ionized impurity scattering. Two implantation species were used for comparison—Cd as a p-type dopant and Sn, typically an n-type dopant, although potentially amphoteric. We find indications of active p-type (Cd) dopant densities substantially exceeding  $10^{19}/\text{cm}^3$ , with no indication of a surface depletion layer and decreasing activation with increasing annealing pulse fluence. For Sn implantations the behavior is rather different. The Raman spectra depend strongly on the annealing pulse energy density between 0.07 J/cm<sup>2</sup> and 1.6 J/cm<sup>2</sup> with evidence of an L<sup>-</sup> coupled mode, a surface depletion layer, and increasing carrier activation from energy densities of 0.3 J/cm<sup>2</sup> through 1.6 J/cm<sup>2</sup>.

Cr-doped semi-insulating GaAs wafers with (001) surfaces were implanted at room temperature with Cd ions at 100 keV and Sn at 180 keV with

doses of  $2 \times 10^{15}$ ,  $5 \times 10^{15}$  and  $10 \times 10^{15}/\text{cm}^2$ . Pulsed laser annealing was performed with a Nd:YAG-pumped dye laser ( $\lambda = 565 \text{ nm}$ ) which provided a smooth, near-Gaussian intensity profile after weak focusing to a spot diameter on the sample of 0.8 mm. Smooth surfaces were retained until very near the damage threshold ~1.5 J/cm<sup>2</sup> and thus no beam homogenization techniques were used. Samples were annealed with the beam incident at 40° from normal with single shots to produce well separated anneal spots with energy densities ranging from 0.057 J/cm<sup>2</sup> to 1.6 J/cm<sup>2</sup>. Pulsed laser energy density at the center of the spot was measured with a 200  $\mu\text{m}$  pinhole in the sample position followed by a disc calorimeter. Quoted energy densities include the  $\cos(40^\circ)$  factor. Above ~0.8 J/cm<sup>2</sup> a visible light flash and audible sound were observable at the GaAs surface during the laser firing.

Raman spectra were obtained with the 514.5 nm and 457.9 nm lines of an Ar<sup>+</sup> laser with typically 100 mW of power incident at ~45 degrees. The laser light polarization was parallel to the horizontal plane of incidence. Scattered light was analyzed for both horizontal and vertical components. Incident and scattered polarizations, except where indicated otherwise, were (x', x') and (x', y') where x' = [110] and y' = [110].

In order to verify that the ~50  $\mu\text{m}$  Raman laser probe was centered on each anneal spot a spatial scan was made in both vertical and horizontal directions with a computer-controlled, stepper-motor-driven stage. In this way the center of each spot was identified and all spectral scans presented below were taken at that location. The spatial scans were obtained with 13 cm resolution with the spectrometer positioned near the frequency of the longitudinal optical (LO) phonon (294 cm<sup>-1</sup>) and the transverse optical (TO) phonon (272 cm<sup>-1</sup>) in undoped GaAs.

The projected ranges of 100 keV Cd and 180 keV Sn ions in GaAs are respectively 30 nm and 47 nm. Thus for a dose of  $5 \times 10^{15}/\text{cm}^2$  the

average impurity density before annealing would be  $\sim 1-2 \times 10^{21}/\text{cm}^3$ . For near-threshold pulsed annealing, where the liquid phase just penetrates beyond the amorphized layer, one expects little additional dopant diffusion and thus a similarly high dopant density after annealing. However for higher pulse energies significant ion diffusion may be expected and consequently lower dopant densities. Free carrier concentrations may be less if large numbers of dopant ions are electrically inactive. The Raman spectra discussed below provide a qualitative estimate of the degree of electrical activity.

Figure 1 shows the Raman spectra of the  $5 \times 10^{15}/\text{cm}^3$  Cd-implanted sample for a wide range of anneal energies. In Raman scattering from a (001) GaAs surface only LO phonons are normally allowed. However, the spectra are dominated by one broad peak located near the TO phonon position in undoped GaAs. We believe this peak is due to the  $L^-$  phonon-plasmon coupled mode fully screened by the high free carrier density.<sup>1</sup> At carrier concentrations above  $\sim 1 \times 10^{19}/\text{cm}^3$  the  $L^-$  mode typically appears at the TO phonon frequency because the long range electric field of the LO phonon is essentially fully screened.

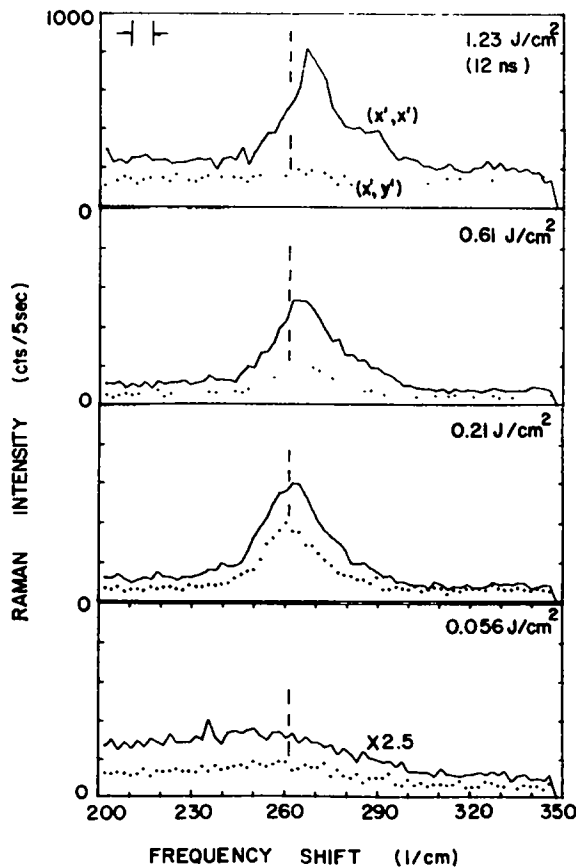


Fig. 1. Raman spectra ( $\lambda=457.9$  nm) of Cd-implanted GaAs,  $5 \times 10^{15}/\text{cm}^3$ , for four different pulsed laser anneal energies. Polarizations are  $(x', x')$  - solid curve and  $(x, y)$  - dotted curve; spectrometer resolution is shown by the vertical bars in the upper left. Dashed vertical line at  $262\text{cm}^{-1}$  indicates the peak position near the epitaxial regrowth threshold.

The peaks of Fig. 1, however, are unusually broad ( $272\text{cm}^{-1}$ ). This suggests that an impurity-induced mechanism is important, similar to that identified for heavy Zn-doped GaAs.<sup>4</sup>

At carrier densities of  $4 \times 10^{19}/\text{cm}^3$  and above, Olego & Cardona<sup>4</sup> interpreted similar peaks as arising from the  $L^-$  modes of the completely screened LO phonons. Normal polarization selection rules for the LO phonon were invalidated because an ionized impurity-induced, wave vector non-conserving mechanism dominated the Raman scattering. In Zn-doped GaAs<sup>4</sup> the phonon frequency decreased monotonically and the width increased with increasing Zn density up to the doping limit of  $9 \times 10^{19}/\text{cm}^3$ .

The shifts and broadenings we observe are even larger. Thus at  $0.21\text{J}/\text{cm}^2$  the TO-like peak is shifted  $10 \pm 2\text{cm}^{-1}$  below its normal position in undoped GaAs. This compares with a maximum shift of  $-5\text{cm}^{-1}$  observed in Ref. 4 for a sample with a hole concentration of  $9 \times 10^{19}/\text{cm}^3$ . Similarly the linewidth is  $17 \pm 2\text{cm}^{-1}$  which again suggests ionized acceptor concentrations well above  $1 \times 10^{19}/\text{cm}^3$ . However, as the annealing energy is increased the Raman peak frequency shift rises and the linewidth decreases indicating reduced ionized impurity scattering. At  $1.2\text{J}/\text{cm}^2$  the shift of  $-3\text{cm}^{-1}$  and width of  $-8\text{cm}^{-1}$  are both consistent with carrier concentrations in the mid- $10^{19}$  range.

More precise estimates of carrier concentrations are not possible at this point since Raman data on extremely heavily doped p-type GaAs are available only for Zn-doping and only up to hole concentrations of  $9 \times 10^{19}/\text{cm}^3$ . The possible dependence of ionized impurity scattering on dopant specie is presently unknown. Furthermore the behavior of peak shift, width and polarization is unknown for dopant densities above  $1 \times 10^{20}/\text{cm}^3$ .

The activation of n-type ion-implanted dopants in GaAs, whether by conventional furnace anneal or by pulsed laser annealing, is much more difficult than for p-type dopants. Thus available Raman data<sup>4</sup> are limited to samples with electron concentrations of  $\leq 1.6 \times 10^{19}/\text{cm}^3$ . The lack of data at higher concentrations makes definitive interpretation of the Raman spectra difficult but several features can be identified.

In Figure 2 we show Raman spectra obtained at  $\lambda = 457.9$  nm for several laser anneal energies from a sample implanted with  $5 \times 10^{15}$  Sn/ $\text{cm}^2$  at 180 keV. The behavior of the spectra is more complex than the case of the Cd-implanted sample discussed above. This behavior may be related to the potentially amphoteric nature of Sn as a dopant in GaAs and the difficulties of achieving high carrier activation of species such as Sn or Si which are typically n-type. We believe that most features of the data may be understood in terms of phonon-plasmon coupled modes in the "bulk"<sup>1</sup> and a surface carrier depletion layer.<sup>2</sup>

The spectra of Fig. 2 show an abrupt transition between anneal fluences of  $0.2\text{J}/\text{cm}^2$  and  $0.3\text{J}/\text{cm}^2$ . The abrupt disappearance of the TO-like peak near  $270\text{cm}^{-1}$  is a clear indication that epitaxial regrowth has occurred. (At  $0.21\text{J}/\text{cm}^2$  and below, this peak arises from TO scattering from polycrystalline grains not having a (001) surface orientation.) Below  $0.3\text{J}/\text{cm}^2$ , the polarization exhibited by the LO-like peak near  $290\text{cm}^{-1}$  would be consistent with its having an origin via an impurity-induced Fröhlich coupling mechanism.<sup>4,5</sup> This forbidden Fröhlich electron-phonon coupling would produce diagonal scattering

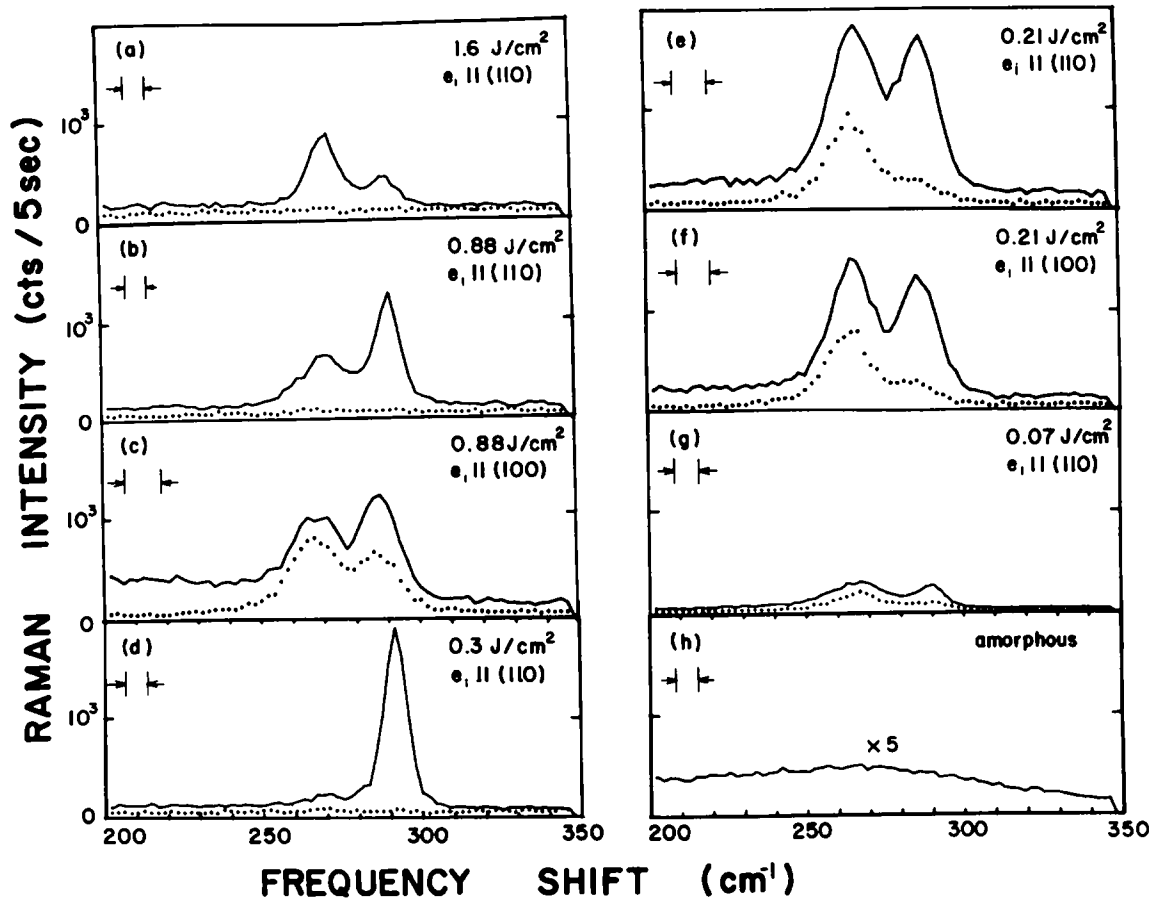


Fig. 2. Raman spectra of Sn-implanted GaAs,  $5 \times 10^{15}/\text{cm}^2$  for several anneal energies. Resolution is indicated by the vertical bars in each trace. Polarizations as in Fig. 1 except for (c) and (f) where sample has been rotated by  $45^\circ$  so that solid curve is (x,x) and dotted curve is (x,y);  $\lambda=457.9$  nm.

which would be independent of sample orientation, i.e.,  $e \parallel e_i$ , where  $e$  and  $e_i$  are the scattered and incident polarizations respectively. We have verified this behavior by rotating the sample  $45^\circ$  about its normal so that  $e = [100]$ ,  $e_i = [010]$  and find also in this case  $(x,x)$  scattering exceeds  $(x,y)$ . See traces (c) and (f) in Fig. 2. Note that the normal Raman-allowed scattering would require  $(x,y)$  scattering in this case. Similar results have been found for LO peaks in heavily doped p-GaSb and p-InSb.<sup>9</sup>

At  $0.3 \text{ J/cm}^2$  and above, the LO-like mode at  $\sim 292 \text{ cm}^{-1}$  gradually decreases in strength with increasing anneal energy. This suggests that its origin lies in a surface depletion layer which is decreasing in thickness due to increasing carrier activation with increasing anneal energy. This is consistent with its origin being related to ionized impurity scattering since in the space charge region the full ionic coulomb potential is realized. However, in the underlying region of high carrier activation the impurity potential will be truncated by the Thomas-Fermi screening of the free carriers.

Above  $0.3 \text{ J/cm}^2$  the TO-like mode at  $\sim 272 \text{ cm}^{-1}$  increases in strength with increasing anneal energy. Its polarization characteristics are consistent with those expected from the  $L^-$  component of the plasmon-LO phonon coupled modes originating in the region of high carrier activation below the surface depletion layer. Thus, the behavior of both peaks is consistent with a gradually increasing carrier activation with pulsed laser anneal energies up to a factor of five above the epitaxial regrowth threshold. Similar behavior was also noted in picosecond pulse annealing of InP.<sup>10</sup> Tell, et al.<sup>10</sup> suggest that the improved electrical activation at high energies may result from a reduced cooling rate.

The present work has not shown an upper limit to the optimum laser annealing energy for activating the Sn-implanted samples. Higher pulse energies were not used because of plasma formation at the sample surface during the laser pulse and visual evidence of a textured (rippled) surface at these high energies. We feel it is possible that the presence of this dense gas or plasma immediately above the GaAs surface may

also be a factor in improving the anneal by improving the near surface stoichiometry.

For electron concentrations above  $\sim 5 \times 10^{17}/\text{cm}^3$  the position of the  $L^-$  mode is insensitive to carrier concentration and is located at the fully screened value equal to the normal TO position ( $272 \text{ cm}^{-1}$ ). A clearer indication of carrier density could be obtained from observations of the position of the  $L^+$  mode in Raman scattering<sup>1</sup>, but we have not found such a peak using laser wavelengths of either 457.9 nm or 514.5 nm. However, comparison of the relative peak heights from the 1.6 J/cm<sup>2</sup> anneal with spectra from bulk doped samples indicates a carrier density slightly above  $1 \times 10^{18}/\text{cm}^3$ . The ratio of peak heights of the TO-like to LO-like modes is a strong function of the laser penetration depth. With 514.5 nm excitation the  $L^-$  peak is enhanced because of the deeper light penetration. Both wavelengths indicate a depletion width of  $\sim 100 \text{ \AA}$  which on a simple Schottky-barrier model<sup>11</sup> requires a carrier concentration of  $\sim 2 \times 10^{18}/\text{cm}^3$ .

The results of this study indicate a vast difference in the pulsed laser annealing behavior between these n-type and p-type dopants in GaAs. The behavior follows trends observed with conventional doping methods, e.g., the difficulty of obtaining heavy n-type dopant concentrations in GaAs. The observation of a surface depletion layer in n-type GaAs but not in p-type again is

consistent with the known behavior of surface defect state pinning of the Fermi level.<sup>12</sup>

Results obtained on samples with the lower implantation dose ( $2 \times 10^{18}/\text{cm}^2$ ) and the higher dose ( $1 \times 10^{19}/\text{cm}^2$ ) exhibit qualitatively similar annealing behavior. The data indicate low activation of Sn dopants (we estimate a maximum of 2% activation) but clearly show increasing activation with annealing fluences well above the epitaxial regrowth threshold. Cd implants appear to be activated easily to densities near  $10^{21}/\text{cm}^3$ . The behavior of the Raman spectra appears to follow the trends observed in heavy Zn-doped GaAs. In order to clarify the origin of the effects displayed in the Raman spectra, measurements are now being made of the dopant and carrier profiles by the use of Rutherford back-scattering techniques and electrical profiling techniques. These methods require larger annealed areas, however, and thus are less suited for the wide survey of annealing pulse energies which is rapidly and non-destructively accomplished with the Raman techniques used here.

*Acknowledgements* - The partial support of the U.S. Office of Naval Research in the early phases of this work is gratefully acknowledged. Thanks are expressed also to Prof. C.M. Sorensen for the emergency use of an Ar laser for part of this work.

#### References

1. See, for example G. Abstreiter, M. Cardona, and A. Pinczuk in *Light Scattering in Solids IV* (Springer Topics in Applied Physics Vol. 54) (Springer, New York, 1984) p. 5; G. Abstreiter, E. Bauser, A. Fischer & K. Ploog, *Appl. Phys.* **16**, 345 (1978); H.J. Stolz & G. Abstreiter, *J. Vac. Sci. & Tech.* **19**, 380 (1981).
2. K.K. Tiong, P.M. Amirtharaj, F.H. Pollak, and D.E. Aspnes, *Appl. Phys. Lett.* **44**, 122 (1984).
3. R. Tsu, J.E. Baglin, G.L. Lasher, J.C. Tsang, *Appl. Phys. Lett.* **34**, 153 (1979); J.F. Morhange, G. Kanellis & M. Balkanski, *J. Phys. Soc. Jpn.* **49**, 1295 (1985); D.E. Aspnes, S.M. Kelso, C.G. Olson, & D.W. Lynch, *Phys. Rev. Lett.* **48**, 1863 (1982); T. Nakamura & T. Katoda, *J. Appl. Phys.* **53**, 5870 (1982).
4. D. Olego & M. Cardona, *Solid St. Commun.* **32**, 375 (1979); *Phys. Rev. B* **24**, 7217 (1981).
5. D.E. Aspnes & A.A. Studna, *Phys. Rev. B* **27**, 985 (1983).
6. M. Balkanski, J.F. Morhange, & G. Kanellis, *J. Raman Spectrosc.* **10**, 240 (1981); J. Sapriel & Y.I. Nissim, *Mat. Res. Soc. Symp. Proc.* **23**, 713 (1984); A. Compaan, G. Contreras, & M. Cardona, *Mat. Res. Soc. Symp. Proc.* **23**, 117 (1984).
7. J.F. Gibbons, W.S. Johnson, & S.W. Mylorie, *Projected Range Statistics Semiconductors and Related Materials* (2nd ed.) (Dowden, Hutchinson, & Ross, Stroudsburg, PA, 1975).
8. G. Abstreiter, R. Trommer, M. Cardona, and A. Pinczuk, *Solid State Commun.* **30**, 703 (1979); R.J. Nicholas & H.J. Stolz, *Sol. St. Electron.* **25**, 55 (1981).
9. R. Dornhaus, R.L. Farrow & R.K. Chang, *Sol. St. Commun.* **35**, 123 (1980).
10. B. Tell, J.E. Bjorkholm & E.D. Beebe, *Appl. Phys. Lett.* **43**, 655 (1983).
11. U.W. Nowak, W. Richter & G. Sachs, *phys. stat. sol. (b)* **108**, 131 (1981).
12. W.E. Spicer, P. Skeath, C.Y. Su & I. Lindau, *J. Phys. Soc. Jpn.* **49** (1980), Suppl. A p. 1079.